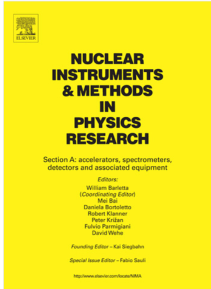

Development of a lithium fluoride zinc sulfide based neutron multiplicity counter

Christian Cowles, Spencer Behling, Phoenix Baldez, Micah Folsom, Richard Kouzes, Vladislav Kukharev, Azaree Lintereur, Sean Robinson, Edward Siciliano, Sean Stave, Patrick Valdez

PII: S0168-9002(18)30029-9
DOI: https://doi.org/10.1016/j.nima.2018.01.015
Reference: NIMA 60440

To appear in: *Nuclear Inst. and Methods in Physics Research, A*

Received date : 9 October 2017
Revised date : 4 January 2018
Accepted date : 5 January 2018

Please cite this article as: C. Cowles, S. Behling, P. Baldez, M. Folsom, R. Kouzes, V. Kukharev, A. Lintereur, S. Robinson, E. Siciliano, S. Stave, P. Valdez, Development of a lithium fluoride zinc sulfide based neutron multiplicity counter, *Nuclear Inst. and Methods in Physics Research, A* (2018), https://doi.org/10.1016/j.nima.2018.01.015

Development of a Lithium Fluoride Zinc Sulfide Based Neutron Multiplicity Counter

Christian Cowles[a,b,*], Spencer Behling[a], Phoenix Baldez[c], Micah Folsom[d], Richard Kouzes[a], Vladislav Kukharev[a], Azaree Lintereur[a,e], Sean Robinson[a], Edward Siciliano[a], Sean Stave[a], Patrick Valdez[a]

[a]*Pacific Northwest National Laboratory, Richland WA*
[b]*Idaho State University, Pocatello ID*
[c]*New Mexico University, Albuquerque NM*
[d]*University of Tennessee, Knoxville TN*
[e]*University of Utah, Salt Lake City UT*

Abstract

The feasibility of a full-scale lithium fluoride zinc sulfide (LiF/ZnS) based neutron multiplicity counter has been demonstrated. The counter was constructed of modular neutron detecting stacks that each contain five sheets of LiF/ZnS interleaved between six sheets of wavelength shifting plastic with a photomultiplier tube on each end. Twelve such detector stacks were placed around a sample chamber in a square arrangement with lithiated high-density polyethylene blocks in the corners to reflect high-energy neutrons and capture low-energy neutrons. The final system design was optimized via modeling and small-scale test. Measuring neutrons from a ^{252}Cf source, the counter achieved a 36% neutron detection efficiency (ϵ) and an 11.7 μs neutron die-away time (τ) for a doubles figure-of-merit (ϵ^2/τ) of 109. This is the highest doubles figure-of-merit measured to-date for a ^{3}He-free neutron multiplicity counter.

Keywords: LiF/ZnS, neutron multiplicity counter, neutron coincidence counter, ^{3}He-free

*Corresponding author
Email address: christian.cowles@pnnl.gov (Christian Cowles)

1. Introduction

Neutron multiplicity counting is a non-destructive assay technique that relies on time correlation between detected neutrons to characterize aspects of neutron emitting samples [1, 2]. Neutron multiplicity counters (NMCs) have historically used ^{3}He as the neutron detecting material because ^{3}He has: a large (n, p) cross section for thermal neutrons, high gamma-ray-to-neutron distinguishability, and ^{3}He is non-toxic and non-corrosive. NMCs built with ^{3}He proportional-counter tubes are mature and reliable technology that have been in deployment for many years [3, 4]. A desire to reduce the time requirements for non-destructive assay of fissile samples along with the recent concern about continued availability of ^{3}He prompted investigation into alternative detectors for neutron multiplicity counting [5, 6].

NMCs are used to determine plutonium mass, neutron self-multiplication, and the ratio of (α, n) to fission neutrons of plutonium-containing samples [7]. Different NMCs have different performance characteristics and may be optimized for specific assay applications, but they are often compared to each other with a doubles figure-of-merit (FOM) based on neutron detection efficiency (ϵ) and neutron die-away time (τ) and is defined for this paper as ϵ^2/τ [8] .

A full-scale lithium fluoride zinc sulfide based neutron multiplicity counter (LiNMC) was constructed and characterized. The LiNMC design was most influenced by the Epithermal Neutron Multiplicity Counter (ENMC) [3], the current highest performing NMC. For example, the LiNMC was designed to occupy the same footprint. Though not known at the time of development, the LiNMC independently adopted similar features to a previous lithium-based neutron coincidence counter designs [9]. The LiNMC's ϵ, τ, and FOM were determined using ^{252}Cf neutron sources. Another quantity of interest in the development of ^{3}He-free detectors is the gamma-ray sensitivity or in other words the number of gamma-ray induced events that are spuriously counted as neutron induced events (ϵ_γ). The gamma-ray sensitivity of the system was determined using ^{137}Cs and ^{60}Co gamma-ray sources. The effect of the gamma-ray sensitivity on the measurement of τ and ϵ was negligible, though its effect on plutonium mass determination must be taken into account [10]. The purpose of this paper is to report the construction of a full-scale LiF/ZnS based NMC and its performance characteristics and compare it with other currently available NMC systems.

2. Design and Construction

Initial LiNMC development was based on Monte-Carlo N-Particle (MCNP) [11] simulations of the ENMC and was then modified to account for the LiF/ZnS technology. These modifications included changing the system from a circular symmetry to square symmetry, replacing the ^{3}He proportional tubes with LiF/ZnS and WSP sheets, reducing the HDPE in the detector regions, implementing modules to hold the detector regions, and implementing lithiated HDPE in the corners. Development followed an iterative process between simulation and experimental measurement, with the most promising designs being kept and refined. Designs were generally kept that increased ϵ or reduced τ to maximize the FOM, or that reduced ϵ_γ.

The core neutron detecting component of the LiNMC is a stack of EJ-426HD LiF/ZnS sheets and EJ-280 wavelength shifting polyvinyl toluene plastic (WSP). Each stack uses five sheets of 0.5 mm thick LiF/ZnS material with 0.5 mm of polyester backing on each side. The LiF/ZnS material is composed of $\approx$10 μm diameter grains of LiF and ZnS suspended in a hydrogenous binder. The Li used in the manufacturing was enriched to 95% ^{6}Li. These five neutron detecting sheets were sandwiched between WSP. The four interior pieces of WSP are 7.0 mm thick and the two exterior pieces 3.5 mm thick. The EJ-426HD LiF/ZnS sheets and EJ-280 WSP sheets were both produced by Eljen (Eljen Technology, Sweetwater, TX). Each stack had a 9821B Series PMT (Electron Tube Enterprises, Uxbridge, UK) on each end and was optically isolated to eliminate inter-stack cross talk. These detector elements are visually depicted in Fig.1 and Fig.2.

The LiNMC uses three detector stacks in each of four light tight modules

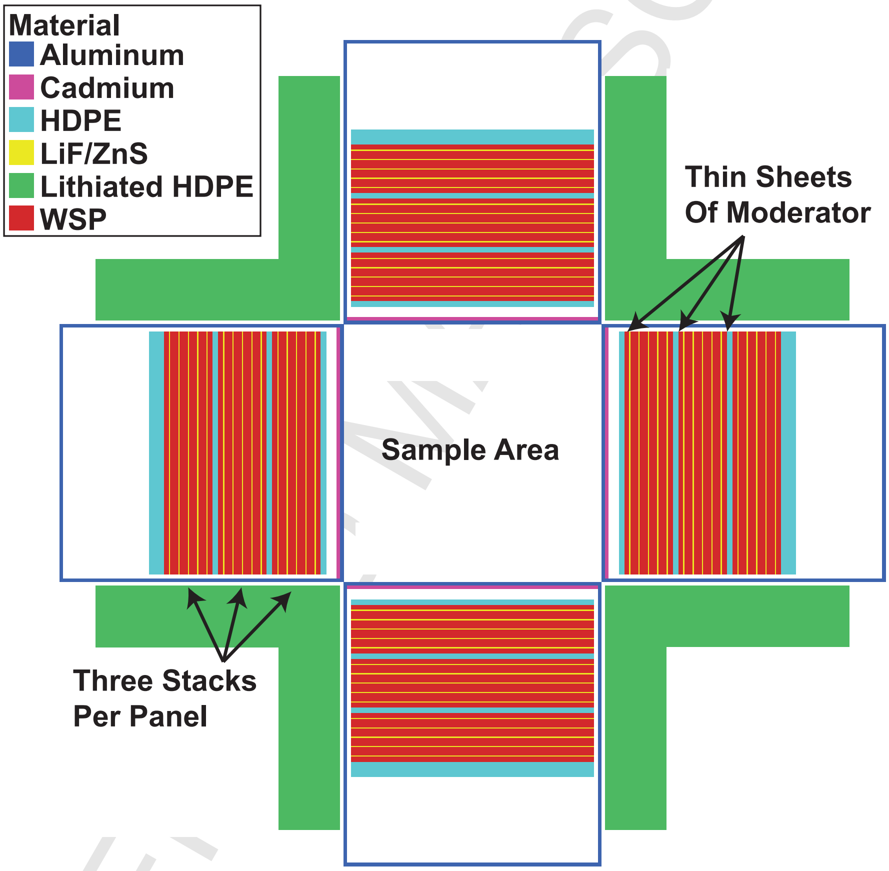

Figure 1: A to-scale schematic of a horizontal slice through the center of the detector. The aluminum panel boxes where designed to accommodate up to four detector stacks. The as-built detector report in this work has only three detector stacks per panel as shown in the figure.

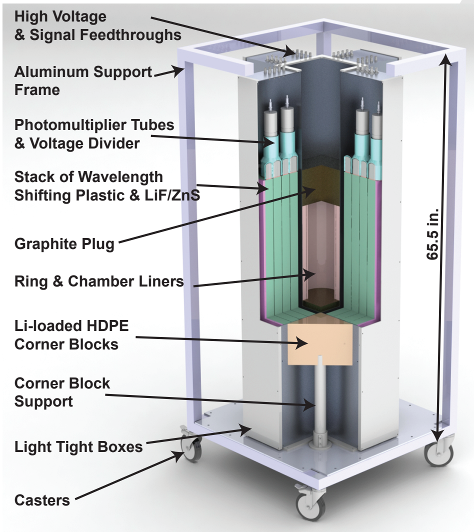

(a) Labeled cutaway render.

(b) Picture of the detector as built.

Figure 2: Two views of the detector. Panel (a) is a schematic view with both exterior and interior elements labeled. Panel (b) shows the actual device with the data acquisition computer hooked up to one panel and an overhead gantry to aid in inserting samples.

arranged around a 20.3 cm wide by 20.3 cm deep by 71.0 cm high sample chamber. The sample chamber utilizes a vertically adjustable sample stand and is completely surrounded with 0.51 mm thick cadmium. 15.2 cm graphite plugs are placed above and below the sample chamber, and the corners of the LiNMC are filled with stacks of (7.56 weight% natural lithium) high-density polyethylene (HDPE) blocks from Shieldwerx (Bladewerx LLC, Rio Rancho, NM) in an "L" configuration 77.0 cm tall, and 5.1 cm thick, with 20.3 cm long arms. The purpose of this design choice is to moderate and reflect fast neutrons into the detector stacks while eliminating the slowest neutrons. The lithiated HDPE is a highly cost effective means of increasing ϵ and reducing τ.

The neutron detection process of the counter begins with the capture of a thermal neutron by the ^{6}Li. The resultant triton and alpha particles exit the micron sized LiF grain, traverse a low Z binder material and excite a fluorophore grain of silver activated ZnS. The scintillation light from the relaxation of the ZnS is absorbed and re-emitted by the WSP leading to more efficient transport of photons to the end of each stack than relying solely on total internal reflection. At the end of each stack a PMT collects the light and produces a signal that is fed directly into the data acquisition system. Placing PMTs on both ends of the detector stacks allowed for improved discrimination between neutron and gamma-ray events since neutron captures tend to produce sufficient scintillation light to be detected by both PMTs, whereas gamma rays tend to produce insufficient scintillation light to be detected by both PMTs.

Signals from the PMTs were digitized by 125 Msps (Linear Technology) analog-to-digital converters (ADCs) mounted on an FM116 peripheral board. The digitized waveforms were processed by a Kintex-7 field programable gate array (FPGA) (Xilinx, San Jose, CA) installed on a on a PC720 PCIe slot card. Both the FM116 and PC720 boards were manufactured by 4DSP LLC, Austin, TX. The firmware running on the FPGA was written in house to distinguish neutron induced events from gamma-ray events. A pulse rate filter was developed for this purpose. The filter counts instances of the PMT signal going over a threshold within an adjustable time window. The filter takes advantage of the observation that gamma-ray induced events tend to have a smaller number of very short pulses compared to neutron induced signals. As the data streams through the time window, the pulse-rate filter checks the current time steps and increments the pulse-rate value if the data entering the time window is above the pulse height threshold and decrements the pulse rate value if the data exiting the time window is above the pulse height threshold. A threshold is placed on this rate filter value to suppress gamma-ray and electronic-noise signals. A visualization of the filter operation is shown in Fig. 3. Only timestamps from neutron induced events were read out via the PCIe bus to a linux computer where a program imposed coincidence between the upper and lower PMTs of each stack and feed the results into a virtual shift register. List mode neutron timing data like, that output by the system has the advantage over using a hardware shift register in that it can be analyzed using different gate lengths making statistics, such as the neutron die-away time in the system easy to measure [12]. This data was evaluated with methods recommended in the Passive Neutron Multiplicity Counting chapter of the Passive Nondestructive Assay Manual [13], which use single, double, and triple neutron count rates to determine sample properties, including plutonium mass. The analysis was performed with a pre-delay value of 0 μs, gate vale of 32 μs, and plutonium sources values of vs1 = 2.154, vs2 = 3.789, vs3 = 5.221, vi1 = 2.879, vi2 = 6.773, and vi3 = 12.630.

3. Characterization

PMT calibrations were conducted to ensure equal performance between all detector stacks. PMTs were roughly voltage matched by placing a LiF/ZnS sheet against their faces, placing each PMT and LiF/ZnS sheet in an HDPE cave with a ^{252}Cf neutron source, and recording the PMT signal rate as a function of applied voltage. All PMTs had their voltages set to provide identical count rate performance based on the HDPE cave results, and PMTs with similar voltage settings were paired to the same detector stack. Fine voltage adjustments were made by placing a ^{252}Cf source in the center of the LiNMC and adjusting each

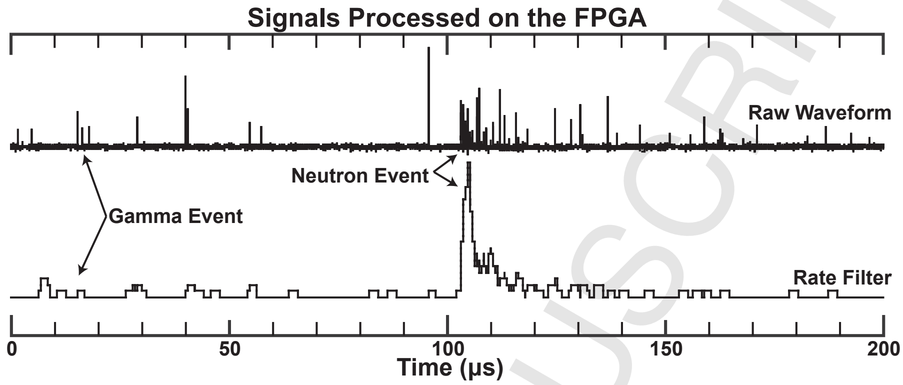

Figure 3: The top trace is the waveform from a single channel of the detector as it experiences a gamma and neutron capture events. The waveform is sampled every 8 ns by the ADC. The bottom trace is the result of running the rate filter algorithm on the raw waveform. A threshold is placed on this filtered output to suppress gamma-ray induced events and trigger on neutron induced events.

PMT's voltage until both PMTs in a pair produced the same signals rate, and each pair produced the same coincidence signal rate as each other pair in a symmetric location in the detector. These voltage settings were maintained for LiNMC characterization measurements.

The neutron detection efficiency, ϵ, was measured with an 8.23 μCi ($3.18 \times 10^4 \pm 7 \times 10^2$ neutrons/s) steel encapsulated ^{252}Cf source at the center of the sample chamber. Data were recorded for 30 minutes, followed by 30 minutes of background, to provide a background subtracted rate. This calibration resulted in $\epsilon = 36 \pm 1\%$. Source activity and uncertainty were determined from an in-house assay that was decay corrected to the measurement day accounting for the contribution of appropriate branching ratios.

The neutron die-away time, τ, was determined by measuring time correlated events from the same ^{252}Cf source. Data were recorded for 30 minutes and a histogram of neutron doubles rates as a function of the coincidence-time window was generated. An exponential function was fit to these data, where the constant of the exponential was taken as τ. This calibration resulted in $\tau = 11.7 \pm 0.1$ μs.

Gamma-ray detection efficiency was measured with a combination of ^{137}Cs and ^{60}Co sources (1.08×10^6 γ/s total), as surrogates for a fission gamma-ray source, at the center of the sample chamber. Coincidence data were recorded for 12 hours, followed by an equal length background measurements. The range of measured gamma-ray detection efficiency is 10^{-3} to 10^{-4}. Small changes to DAQ settings, particularly rate filter algorithm parameters, tended to have minimal effects on ϵ and τ measurements, but order-of-magnitude sized effects on gamma-ray detection efficiencies.

These measured values were used to calculate a LiNMC FOM of 110 ± 6, where ϵ is in percent and τ is in μs. LiNMC performance results are compared to other constructed ^{3}He and ^{3}He-free neutron multiplicity counters in Table 1. In addition to measurements of the detector properties a plutonium mass assay was conducted with minimal DAQ tuning. The accepted Pu mass was 104.1 g and the LiNMC assay mass was 95.9 ± 6.6 g. The assay was 6.3 ± 2.5 % lower than the accepted Pu mass. This calibration result was based on singles, doubles, and triples rates of 4211 Hz, 471.8 Hz, and 43.48 Hz respectively [13]. A systematic study of the detector response with respect to neutron source type and activity was beyond the scope of this study.

4. Conclusion

The LiNMC is the highest performing ^{3}He-free neutron multiplicity counter, in terms of doubles figure-of-merit, at the time of this writing and has shown very promising preliminary results for development into a deployable system for safeguard applications, including material verification, accountancy, and identification. The LiNMC's basic components have been brought together and validated and provide strong evidence that LiF/ZnS is a viable material for development of high performance ^{3}He-free neutron detectors, including neutron multiplicity counters.

Lithium-based neutron detectors may be a high performance alternative to ^{3}He for neutron multiplicity counting. ^{3}He neutron detectors have been opti-

Neutron Counter	ϵ (%)	τ (μs)	FOM
^{3}He Based Systems			
ENMC [14]	65	22	192
Inventory Sample Verification System [15]	31–42	45	21–39
High Level Neutron Coincidence Counter [15]	17.5	43	7.1
Uranium Neutron Coincidence Collar I [15]	16	59	4.3
Uranium Neutron Coincidence Collar II [15]	15.4	59	4.0
^{3}He Free Systems			
LiNMC (this work)	36	11.7	110
Water-Based Well Counter [16]	28	16	49
†LiF/ZnS High Level Neutron Coincidence Counter [15, 8]	25.4	31	20.8
†LiF/ZnS Uranium Neutron Coincidence Collar [15]	18.7	18	19.4
Novel LiF/ZnS Neutron Multiplicity Counter [9]	37	83	16
†Boron Straws Detector [8]	26	50	13.5
†BF_3 Based Neutron Correlation Counter [15]	28.7	73.7	11.2
†BF_3 Proportional Tubes [8]	26	85	8.0
Boron-Coated Straw Based Neutron Coincidence Counter [15, 8]	13.6	26.0	7.1
High Level Neutron Counter – Boron [15]	18.8	75	4.7
^{10}B-Lined Proportional Tube Neutron Collar [15]	11.6	75	1.8
LiF/ZnS Based High Level Neutron Coincidence Counter [15, 8]	8.5	52	1.4

† Predicted values based on modeling

Table 1: Doubles figure-of-merit performance comparison between LiNMC and other neutron multiplicity counterss.

mized over many decades, whereas lithium-based neutron multiplicity counting is an emerging technology with many avenues for potential improvement. Future LiNMC development is anticipated to increase the FOM by increasing ϵ and/or reduce τ. It has been demonstrated through modeling and limited testing that this could be accomplished by 1) replacing the four lithiated HDPE "L" blocks with four more modules of detector stacks, 2) increasing the LiF/ZnS sheet packing density, 3) adding a fourth detector stack within each module, and 4) continuing to optimizing materials and geometries for maximum ϵ with minimum τ.

Although the LiNMC's current gamma/neutron discrimination ratio in the range of 10^{-3} to 10^{-4}, is insufficient for many samples, MCNP shielding simulations, and pulse shape discrimination tests indicate that these gamma/neutron discrimination ratio of approximately of 10^{-8} should be achievable. Even lower gamma/neutron discrimination ratios may be achievable through optimizing DAQ settings, particularly the rate filter algorithm, or by sacrificing some neutron detection efficiency. Overall measurements of the current system performance are encouraging and many avenues exist for continued improvement.

5. Acknowledgement

We express our thanks to the office of Defense Nuclear Nonproliferation Research and Development and the Office of International Nuclear Safeguards within the U.S. Department of Energy's National Nuclear Security Administration for funding this work. Pacific Northwest National Laboratory is operated for the U.S. Department of Energy by Battelle under contract SE-AC05-76RLO 1830. This is release PNNL-SA-123198.

References

[1] N. Ensslin, W. C. Harker, M. S. Krick, D. G. Langner, M. M. Pickrell, J. E. Stewart, Application Guide to Neutron Multiplicity Counting, LA-13422-M, Tech. rep., Los Alamos National Laboratory, Los Alamos, NM

(Nov 1998).
URL http://permalink.lanl.gov/object/tr?what=info:lanl-repo/lareport/LA-13422-M

[2] D. Cifarelli, W. Hage, Models for a three-parameter analysis of neutron signal correlation measurements for fissile material assay, Nuclear Instruments and Methods in Physics Research Section A: Accelerators, Spectrometers, Detectors and Associated Equipment 251 (3) (1986) 550–563. doi:10.1016/0168-9002(86)90651-0.
URL http://linkinghub.elsevier.com/retrieve/pii/0168900286906510

[3] H. O. Menlove, C. D. Rael, K. E. Kroncke, K. J. DeAguero, Manual for the epithermal neutron multiplicity detector (ENMC) for measurement of impure MOX and plutonium samples, LA-14088, Tech. rep., Los Alamos National Laboratory, Los Alamos, NM (May 2004).
URL http://www.osti.gov/scitech/servlets/purl/828513

[4] International Atomic Engergy Agency, Safeguards techniques and equipment: 2011 Edition International Nuclear Verification Series No. 1 (Rev. 2).
URL http://www-pub.iaea.org/books/iaeabooks/8695/Safeguards-Techniques-and-Equipment

[5] R. T. Kouzes, The ^{3}He Supply Problem, PNNL-18388, Tech. rep., Pacific Northwest National Laboratory, Richland, WA (May 2009). doi:10.2172/956899.
URL http://www.osti.gov/servlets/purl/956899-IInY7M/

[6] R. T. Kouzes, J. H. Ely, L. E. Erikson, W. J. Kernan, A. T. Lintereur, E. R. Siciliano, D. L. Stephens, D. C. Stromswold, R. M. Van Ginhoven, M. L. Woodring, Neutron detection alternatives to ^{3}He for national security applications, Nuclear Instruments and Methods in Physics Research Sec-

tion A: Accelerators, Spectrometers, Detectors and Associated Equipment 623 (3) (2010) 1035–1045. doi:10.1016/j.nima.2010.08.021.

[7] M. Krick, J. Swansen, Neutron multiplicity and multiplication measurements, Nuclear Instruments and Methods in Physics Research 219 (2) (1984) 384–393. doi:10.1016/0167-5087(84)90349-1.
URL http://linkinghub.elsevier.com/retrieve/pii/0167508784903491

[8] R. D. McElroy, ^{3}He Alternatives Summary Report, ORNL/TM-2015/310, Tech. rep., Oak Ridge National Laboratory, Oak Ridge, TN (Nov 2015). doi:10.2172/1234989.
URL https://www.osti.gov/scitech/biblio/1234989-alternatives-summary-report

[9] J. C. Barton, C. J. Hatton, J. E. McMillan, A novel neutron multiplicity detector using lithium fluoride and zinc sulphide scintillator, Journal of Physics G: Nuclear and Particle Physics 17 (12) (1991) 1885–1899. doi:10.1088/0954-3899/17/12/010.
URL http://www.sciencedirect.com/science/article/pii/S0168900214011760

[10] C. C. Cowles, R. S. Behling, G. R. Imel, R. T. Kouzes, A. T. Lintereur, S. M. Robinson, E. R. Siciliano, S. C. Stave, Effects of Correlated and Uncorrelated Gamma Rays on Neutron Multiplicity Counting, IEEE Transactions on Nuclear Science 64 (7) (2017) 1865–1870. doi:10.1109/TNS.2017.2667407.
URL http://ieeexplore.ieee.org/document/7867089/

[11] J. T. Goorley, M. R. James, T. E. Booth, F. B. Brown, J. S. Bull, L. J. Cox, J. W. J. Durkee, J. S. Elson, M. L. Fensin, R. A. I. Forster, J. S. Hendricks, H. G. I. Hughes, R. C. Johns, B. C. Kiedrowski, R. L. Martz, S. G. Mashnik, G. W. McKinney, D. B. Pelowitz, R. E. Prael, J. E. Sweezy, L. S. Waters, T. Wilcox, A. J. Zukaitis, Initial MCNP6 Release Overview

– MCNP6 version 1.0, LA-UR-13-22934, Tech. rep., Los Alamos National Laboratory, Los Alamos, NM (Jun 2013). doi:10.2172/1086758.
URL https://www.osti.gov/scitech/biblio/1086758-initial-mcnp6-release-overview-mcnp6-version

[12] J. Bagi, L. Dechamp, P. Dransart, Z. Dzbikowicz, J.-L. Dufour, L. Holzleitner, J. Huszti, M. Looman, M. Marin Ferrer, T. Lambert, P. Peerani, J. Rackham, M. Swinhoe, S. Tobin, A.-L. Weber, M. Wilson, Neutron coincidence counting with digital signal processing, Nuclear Instruments and Methods in Physics Research Section A: Accelerators, Spectrometers, Detectors and Associated Equipment 608 (2) (2009) 316–327. doi:10.1016/j.nima.2009.07.029.
URL http://www.sciencedirect.com/science/article/pii/S0168900209014211

[13] N. Ensslin, M. S. Krick, D. G. Langer, M. M. Pickrell, T. D. Reilly, J. E. Stewart, Passive Nondestructive Assay Manual, LA-UR-07-1402, Tech. rep., Los Alamos National Laboratory, Los Alamos, NM (2007).
URL http://www.lanl.gov/orgs/n/n1/panda/

[14] J. E. Stewart, H. O. Menlove, D. R. Mayo, W. H. Geist, L. A. Carrillo, G. D. Herrera, The Ephithermal Neutron Multiplicity Counter Design and Performance Manual: More Rapid Plutonium and Uranium Inventory Verifications by Factors of 5-20, LA-13743-M, Tech. rep., Los Alamos National Laboratory, Los Alamos, NM (Aug 2000). doi:10.2172/775881.
URL https://www.osti.gov/scitech/biblio/775881-jqw8CS/webviewable/

[15] D. Henzlova, R. Kouzes, R. McElroy, P. Peerani, K. Baird, A. Bakel, M. Borella, M. Bourne, L. Bourva, F. Cave, R. Chandra, D. Chernikova, S. Croft, G. Dermody, A. Dougan, J. Ely, E. Fanchini, P. Finocchiaro, V. Gavron, M. Kureta, K. D. Ianakiev, K. Ishiyama, T. Lee, C. Martin, K. McKinny, H. O. Menlove, C. Orton, A. Pappalardo, B. Pedersen,

R. Plenteda, S. Pozzi, M. Schear, M. Seya, E. Siciliano, S. Stave, L. Sun, M. T. Swinhoe, H. Tagziria, J. Takamine, A. L. Weber, T. Yamaguchi, H. Zhu, Current Status of Helium-3 Alternative Technologies for Nuclear Safeguards, LA-UR-15-21201, Tech. rep., Los Alamos National Laboratory, Los Alamos, NM (Dec 2015).
URL http://permalink.lanl.gov/object/tr?what=info:lanl-repo/lareport/LA-UR-15-21201

[16] S. Dazeley, A. Asghari, A. Bernstein, N. S. Bowden, V. Mozin, A water-based neutron detector as a well multiplicity counter, Nuclear Instruments and Methods in Physics Research Section A: Accelerators, Spectrometers, Detectors and Associated Equipment 771 (2015) 32–38. doi:10.1016/J.NIMA.2014.10.028.
URL http://www.sciencedirect.com/science/article/pii/S0168900214011760